

**CHAPTER VIII**  
**QUIESCENT AND SHEAR-INDUCED MELT CRYSTALLIZATION IN**  
**POLY(TRIMETHYLENE TEREPHTHALATE)**

Phornphon Srimoan, Pitt Supaphol\*, and Anuvat Sirivat

*The Petroleum and Petrochemical college, Chulalongkorn University, Soi Chula 12,  
Phyathai Road, Pathumwan, Bangkok 10330, THAILAND*

**ABSTRACT**

Quiescent and shear-induced melt crystallization of poly(trimethylene terephthalate) PTT was investigated using differential scanning calorimeter and cone and plate rheometer. The simple shear-induced isothermal crystallization model based on assumption that shear stress only shift the equilibrium melting was applied. The parameters from quiescent crystallization model can be directly used in shear-induced crystallization one. Shear stress applied during isothermal crystallization can also increase bulk crystallization rate and shift peak temperature to higher temperature. Avrami analysis was also analyzed isothermal crystallization data of shear untreated and treated samples at different shearing temperature. For non-isothermal crystallization, non-sheared and sheared samples from capillary rheometer also used to study using differential Nakamura model and modified differential Nakamura model to fit the experimental data. Fittings results using differential Nakamura model show better fitting than using modified differential Nakamura one for PTT studied. The effective activation energy based on Friedman method of shear treated sample was found to be lower than that of shear untreated sample at all melt conversion calculated.

**(Key-words:** poly(trimethylene terephthalate); shear-induced crystallization; crystallization kinetics)

---

\*

To whom correspondence should be addressed: Fax: +66-2215-4459; E-mail address: pitt.s@chula.ac.th

## 1. INTRODUCTION

In processing conditions however, polymer melts are generally sheared (i.e., under shear flow) and stretched (i.e., under elongational flow). Crystallization therefore takes place in a molecularly oriented state with in itself may enhance nucleation and crystallization rate. The kinetics of crystallization of polymers in quiescent condition were extensively investigated by many observers but the effect of shear or stress is still not well understand because of difficulties in the experimental measurement and a proper crystallization kinetics model is not available.

Wolkowicz [1] studied the effect of shear on the melt crystallization behavior of poly (1-butene) at several shear rates and degree of under cooling. The shear stress in the system induced a certain amount of nucleation orientation which greatly accelerated the overall crystalline transformation process. Patel and Spruiell [2] proposed extended half-time model including orientational effect to describe on-spline crystallization of nylon-6 and found that their model can only apply in a semiquantitative analysis. Eder *et al.* [3] proposed microscopic model for shear-induced crystallization under isothermal crystallization with a constant shear rate. They proposed that nucleation rate and growth rate were supposed to be functions of orientation in the melt depending on shear rate, shearing time and stress relaxation effect. Jerschow and Janeschitz-Kriegl [4] studied about effect of long molecules in shear-induced crystallization of isotactic polypropylene by using nucleation model based on thread-like precursors which were formed during shear flow. From this experiment, they found that the long polymer molecules had significant effect for the formation of highly oriented layers due to shear treatment and polypropylene with narrow molecular mass distributions had a lower tendency to form this structure.

Recently, Ahn *et al.* [5] studied shear-induced cold crystallization of poly(ethylene terephthalate) under isothermal and non-isothermal conditions. The differential type of Nakamura model, with the nucleation constant  $K_g$  modified with the degree of orientation, was used to fit the experimental results under a non-isothermal condition. The concept of shear-induced crystallization model started with the effect of orientation can reduce entropy or increase the number of nuclei.

Guo and Narh [6] proposed simplified model of stress-induced crystallization kinetics of PET under isothermal crystallization from the melt. The assumption of this model is that the effect of shear stress on crystallization is to increase the equilibrium melting temperature  $T_m^0$ . The advantage of this model is that the parameters in quiescent state crystallization model do not change and can be determined easily. They found that shear stress applied not only increased the rate of crystallization, but also broadened the crystallization temperature range. The peak temperature at highest crystallization rate was also shifted to higher temperature with increasing shear stress.

PTT is now commercially available and has been produced by Shell Chemicals under the tradename Corterra<sup>TM</sup> [7]. There are many papers on crystallization of PTT, but hardly any reports on the effect of stress or shear on crystallization behavior of PTT. The objective of this work is to study the effect of stress on crystallization in the quiescent conditions and to better understand the stress-induced crystallization.

In this manuscript, we focus on the effect of shear on the crystallization kinetics, and the effect of cooling rate on sheared samples using cone and plate rheometer and differential scanning calorimetry (DSC) in both isothermal and non-isothermal crystallization.

## 2. THEORETICAL BACKGROUND

### 2.1. Quiescent Crystallization

The most common approach used to describe the overall isothermal crystallization kinetics is the Avrami equation [8-10]:

$$\theta(t) = 1 - \exp[-(K_a t)^{n_a}] \in [0, 1] \quad (1)$$

where  $K_a$  and  $n_a$  are the Avrami crystallization rate constant and the Avrami exponent, respectively. Equation (1) does not consider the induction time  $t_i$  for the crystallization process in polymers. An empirical relationship between induction time and crystallization temperature is generally used in the form [11]:

$$t_i = t_m (T_m^0 - T_c)^{-a} \quad (2)$$

where  $t_m$  and  $a$  are material constants,  $T_m^\circ$  is the equilibrium melting temperature,  $T_c$  is the crystallization temperature, and  $t_i$  is the induction time at temperature  $T_c$ .

Nakamura *et al.* [12] proposed a model by simplifying Avrami model on the basis of isokinetic conditions and the assumption that the number of activated nuclei is constant. Nakamura developed the following equation from the Avrami theory:

$$\theta(t) = 1 - \exp\left[-\left(\int_0^t K(T) dt\right)^n\right] \quad (3)$$

For process modeling, differentiating Equation (3) and rearranging lead to the differential form of Nakamura equation which is frequently more useful than its integral form as follows:

$$\frac{d\theta}{dt} = nK(T)(1-\theta)[-\ln(1-\theta)]^{(n-1)/n} \quad (4)$$

where

$$K(T) = k(T)^{1/n} = (\ln 2)^{1/n} (1/t_{0.5}) \quad (5)$$

$$(t_{0.5}^{-1}) = (t_{0.5}^{-1})_0 \exp\left(\frac{-U^*}{R(T-T_\infty)}\right) \exp\left(\frac{-K_g}{T\Delta Tf}\right) \quad (6)$$

where  $T$  is the crystallization temperature;  $t_{0.5}$  the time taken for half of the crystallization develop;  $(t_{0.5}^{-1})_0$ , a pre-exponential factor that include all terms independent of temperature;  $R$ , the universal gas constant;  $\Delta T = T_m^\circ - T_c$ , degree of undercooling;  $T_m^\circ$ , the equilibrium melting temperature;  $f = 2T/(T + T_m^\circ)$ , a correction factor accounting for the reduction in the latent heat of fusion as the temperature is decreased;  $T_\infty = T_g - 30$  K, the temperature below which transport ceases;  $T_g$ , the glass transition temperature;  $U^*$ , the activation energy for segmental jump rate in polymer; and  $K_g$ , the nucleation exponent. Equation (12) have often taken to have a similar temperature dependence to that of the subsequent crystal growth rate  $G$  (written in the context of the original Lauritzen-Hoffmann secondary nucleation theory (LH theory) [13]. Patel and Spruiell [2] proposed modified differential Nakamura model. By letting  $Y = \ln(1/(1-\theta))$ , the non-isothermal crystallization rate equation can be written as follows:

$$\frac{dY}{dt} = nK(T)Y^{(n-1)/n} \quad (7)$$

$$K(T) = k(T)^{1/n} = C_1 \exp\left[\frac{-U^*}{R(T-T_\infty)}\right] \exp\left[\frac{-C_2}{T\Delta Tf}\right] \quad (8)$$

where  $C_1$  is equal to  $(\ln 2)^{1/n}(t_{0.5}^{-1})_0$ .

For processes that occur on cooling, reliable values of the effective activation energy can be obtained, for instance, by the differential isoconversional method of Friedman [14]. The Friedman equation is obtained as follows:

$$\ln\left(\frac{d\alpha}{dt}\right)_{\alpha,i} = \ln[Af(\alpha)] - \frac{E\alpha}{RT_{\alpha,i}} \quad (9)$$

where the subscript  $\alpha$  denotes the values related to a given extent of conversion and  $i$  is the ordinal number of the run carried out at the heating rate,  $\beta_i$ . The rate can be conveniently determined from DSC data.

## 2.2. Shear-induced Crystallization

At the melting temperature, the free energy of the crystals equals the free energy of the melt so that the melting temperature may be written as [15]:

$$T_m^0 = \frac{\Delta H_f}{\Delta S_f} = \frac{H_m - H_c}{S_m - S_c} \quad (10)$$

where  $\Delta H_f$  is the heat of fusion,  $\Delta S_f$  is the entropy of fusion,  $H_m$  and  $H_c$  are the enthalpies of the melt and crystalline phases, respectively, and  $S_m$  and  $S_c$  are the entropies of the melt and crystalline phases, respectively.

By assuming that the free energy of the crystalline phase is independent of the applied strain, and that the deformation energy follows Hooke's law, Haas and Maxwell [15] arrived at the following expression for the increased melting point for a stressed polymer melt:

$$T_m = \frac{T_m^0}{\Delta H_f} \left[ \frac{\tau^2}{2G} \right] + T_m^0 \quad (11)$$

where  $T_m$  is the melting temperature under shear stress,  $G$  is the elastic shear modulus of the polymer, and  $\tau$  is the elastic shear stress.

The first term on the right side of Equation (11) can be thought of as the increase in melting temperature that is,

$$T_{\text{shift}} = \frac{T_m^0}{\Delta H_f} \left[ \frac{\tau^2}{2G} \right] \quad (12)$$

It should be noted here that Equation (12) is based on the assumption that shear modulus is independent of the applied shear stress. However, the relationship

between the shear modulus and shear stress is very complicated. Therefore, the melting temperature shift may not necessarily follow Equation (12). Guo and Narh [6] suggested that simple relation between shear stress and equilibrium melting temperature shift in high stress should be constant in high shear rate region (for polymer which have favor conformational as fully extended chain) because orientation of polymer reach a maximum value.

$$T_{\text{shift}} = C_1 e^{\frac{C_2}{\tau}} \quad (13)$$

where  $C_1$  and  $C_2$  are material constants that can be determined directly from the experimental data.

If it is assumed that the effect of stress on the kinetics of crystallization is only by increasing the melting temperature, i.e. by increasing the degree of undercooling, then by replacing  $T_m^\circ$  in Eq. (6) with  $T_m$

$$T_m = T_m^\circ + T_{\text{shift}} \quad (14)$$

and therefore

$$f = \frac{2T}{T + T_m} \quad (15)$$

So, the induction time in shear condition can also be obtained by replacing the equilibrium melting temperature in Equation (2) with  $T_m$ :

$$t_i(T, \tau) = t_m (T_m - T)^{-a} \quad (16)$$

Rearranging Equation (16)

$$T_m = T_c + \left[ \frac{t_m}{t_i(T, \tau)} \right]^{1/a} \quad (17)$$

So the final result, the equilibrium melting temperature shift  $T_{\text{shift}}$  can be readily expressed as

$$T_{\text{shift}} = T_m - T_m^\circ = T_c + \left[ \frac{t_m}{t_i} \right]^{1/a} - T_m^\circ \quad (18)$$

Recently, Ahn *et al.* [5] proposed the kinetic model of shear-induced crystallization can be expressed as Equations (19) and (20) which are modified to crystallization rate constant  $K(T, \tau)$ .

$$\frac{d\theta}{dt} = nK(T, \tau)(1 - \theta)[-\ln(1 - \theta)]^{(n-1)/n} \quad (19)$$

where

$$K(T, \tau) = K_1 \exp\left(\frac{-U^*}{R(T - T_\infty)}\right) \exp\left(\frac{-K_g}{T\Delta T f} \cdot \frac{1}{1 + h(T, \tau)}\right) \quad (20)$$

For overall rate crystallization

$$K(T, \tau) = k(T, \tau)^{1/n} = (\ln 2)^{1/n} (t_{0.5}^{-1}) \quad (21)$$

$$t_{0.5}^{-1} = (t_{0.5}^{-1})_0 \exp\left(\frac{-U^*}{R(T - T_\infty)}\right) \exp\left(\frac{-K_g}{T\Delta T f} \cdot \frac{1}{1 + h(T, \tau)}\right) \quad (22)$$

### 3. EXPERIMENTAL

#### 3.1. Materials

Poly(trimethylene terephthalate) (PTT) were supplied in pellet form by Shell Chemical Company (USA) Ltd. (Corterra CP509201). The weight- and number-average molecular weight of this resin were determined to be ca. 78,100 and 34,700 Daltons, respectively. It should be noted that molecular weight characterization of these resins was carried out by Dr. Hoe Chuah and his co-workers of Shell Chemicals (USA) based on size-exclusion chromatography (SEC) technique.

#### 3.2. Sample Preparation

For shear untreated samples, PTT pellets clear grade were dried in a vacuum oven at 140°C for 5 hours prior to further use. A film of approximately 200 μm in thickness for each resin was melted-pressed at 260°C for PTT in Wabash V50H compression molding machine under an applied pressure of  $4.62 \times 10^2 \text{ MN}\cdot\text{m}^{-2}$ . After 5 min holding time, the film was taken out and allowed to cool at the ambient condition down to room temperature between the two metal platens. This treatment assumes that previous thermo-mechanical history was essentially erased, and provided a standard crystalline memory condition for the as-prepared film.

For disk shape samples, PTT pellets were dried in the oven at 140°C for 5 hours. Then the pellets were put into the mold which circle geometry to compress into the disk shape samples which thickness ca. 1 mm. For high shear rate samples, PTT pellets were dried in the oven at 140°C for 5 hours before filling in the barrel of capillary rheometer. A capillary rheometer (Instron model 4303) was used to applied shear stress to polymer samples before studying shear-induced crystallization. The

diameter of die and L/D ratio are 1.25 mm and 40.15, respectively. Preheat time used was ca. 10 min. When the shear treated sample were extruded pass through capillary die, they were cut and quenched immediately in liquid nitrogen bath. The shearing temperature  $T_s$  used were 250 and 260°C.

### 3.3. Methods

For Rheological measurements were carried out using a cone and plate rheometer (Rheometrics Scientific, model ARES). The disk shape samples were inserted between cone and plate geometry and heated up to a desired fusion temperature at 260°C. When the sample was melted completely, it was cooled to a desired crystallization temperature. Then shear rate was applied to observe the variation of stress as function of crystallization time.

A DSC (DSC-7, Perkin-Elmer) was used to follow isothermal crystallization and subsequent melting behavior of these polyester resins. Calibration for temperature scale was carried out using a indium standard ( $T_m^{\circ} = 156.6^{\circ}\text{C}$  and  $\Delta H_f^{\circ} = 28.5\text{ Jg}^{-1}$ ) on every other run to ensure accuracy and reliability of the data obtained. To minimize thermal lag between polymer sample and DSC furnace, each sample holder was loaded weighing around  $8.0 \pm 0.3$  mg. It is worth noting that each sample was used only once and all the runs were carried out under nitrogen atmosphere to prevent extensive thermal degradation.

Isothermal crystallization from melt of shear untreated and treated samples from capillary rheometer started with heating each sample from 40°C at a heating rate of  $80^{\circ}\text{C}\cdot\text{min}^{-1}$  to a desired fusion temperature  $T_f$  at 260°C. To ensure complete melting, the sample was kept at the respective  $T_f$  for a holding period of 5 min. After this period, each sample was rapidly cooled (i.e., ca.  $200^{\circ}\text{C}\cdot\text{min}^{-1}$ ) from  $T_f$  to a desired crystallization temperature, where it was held until crystallization process was considered complete (when no significant change in the heat flow as a function of time was further observed).

Non-isothermal crystallization from melt of non-sheared and sheared sample from capillary rheometer started with heating each sample from 40°C at a heating rate of  $80^{\circ}\text{C}\cdot\text{min}^{-1}$  to a desired fusion temperature  $T_f$  at 260°C for 5 min.



Then the samples was cooled at different cooling rate to observe melt crystallization exotherms.

## 4. RESULTS AND DISCUSSION

### 4.1. Quiescent Isothermal Crystallization from the Melt

Figure 1 illustrates the induction time  $t_i$  of PTT after isothermal crystallization at different crystallization temperature ranging from  $T_c$  184 to 213°C. It shown that  $t_i$  increased as increased crystallization temperature and shown sharply increased after  $T_c$  ca. 200°C. From the relationship between  $t_i$  and  $T_c$  in Equation (2), it was taken logarithm and rearranged

$$\log t_i = \log t_m - a (\log(T_m^\circ - T_c)) \quad (23)$$

where  $a$  is -slope and  $\log t_m$  is intercept y-axis. Figure 2 shows the plot of  $\log t_i$  versus  $\log(T_m^\circ - T_c)$ . It should be noted here that the value of  $t_i$  used was in range of  $T_c$  198 to 213°C because plot of  $\log t_0$  versus  $T_m^\circ - T_c$  shown the change of slope ca. at 198°C. The value of  $T_m^\circ$  used is 243.6°C [16]. The material constants are  $t_m = 5.62 \times 10^{12} \text{ K}^{8.0} \text{ min}$  and  $\alpha = 8.0$ . An important bulk or overall crystallization kinetic parameter which can be determined directly from the  $\theta(t)$  data is the reciprocal half-times of crystallization  $t_{0.5}^{-1}$ , which is defined as the elapsed time measured from the onset of crystallization until the crystallization is half-completed. According to Figure 3, it is apparent that the reciprocal half-times of crystallization  $t_{0.5}^{-1}$  decreased assumingly exponentially with increasing crystallization temperature  $T_c$ , at least within the temperature range studied. From Hoffmann model [13] in Equation (6), the test of regime can be performed through the plot of  $\log(t_{0.5}^{-1}) + U^*/2.303R(T_c - T_\infty)$  versus  $1/2.303T_c(\Delta T)f$ . This type of plot factors out the contribution of the transport term from the bulk crystallization rate, and the slope is equal to the negative value of the nucleation exponent (i.e., slope =  $-K_g$ ) and  $\log(t_{0.5}^{-1})_0$  is equal to intercept y-axis. From this plot as shown in Figure 4, the temperature at point changing from regime III to II was found to be ca. 200°C. Huang and Chang (2000) also reported temperature change from observation of linear growth rate from microscopic level being ca. 196°C which is closed to value from bulk crystallization rate  $t_{0.5}^{-1}$  in this experiment. For regime III,  $(t_{0.5}^{-1})_{0,III}$  and  $K_{g,III}$  calculated were found to be  $1.15 \times 10^5$

$\text{min}^{-1}$ , and  $1.73 \times 10^5 \text{ K}^2$ , respectively. For regime II,  $(t_{0.5^{-1}})_{0,II}$  and  $K_{g,II}$  calculated were found to be  $1.03 \times 10^5 \text{ min}^{-1}$  and  $1.26 \times 10^5 \text{ K}^2$ , respectively. The  $K_{g,III}/K_{g,II}$  value in PTT was ca. 1.37.

#### 4.2. Shear-induced Isothermal Crystallization from the Melt

For experiment in cone and plate rheometer, the increase of shear stress should be referred to start of crystallization process due to stiffness increased of material. The induction time  $t_i$  in shear condition was decreased when comparing with quiescent condition. The value of  $t_m = 5.62 \times 10^{12} \text{ K}^{8.0} \text{ min}$  and  $a = 8.0$  from quiescent isothermal melt crystallization were substituted in Equation (18) to determine equilibrium melting temperature shift  $T_{\text{shift}}$ . The values of  $t_i$  and calculated  $T_{\text{shift}}$  with different  $T_c$  and shear rate are shown in Table 1. At the same crystallization temperature, the value of  $t_i$  was found to decrease with increasing shear rate. At the same shear rate,  $t_i$  was increased with increasing  $T_c$ . The shear stress versus crystallization time of PTT isothermally crystallized at  $210^\circ\text{C}$  using cone and plate rheometer are shown in Figure 5. The curves of stress versus time were found to be influenced by shear rate. Figure 6 also shows the values of  $T_{\text{shift}}$  as a function of shear stress. Equation (13) was used to fit the calculated values of  $T_{\text{shift}}$  and the best fit obtained with constant  $C_1 = 7.1^\circ\text{C}$  and  $C_2 = 247.9 \text{ Pa}$ . The effect of shear stress on bulk crystallization rate of PTT are shown in Figure 7. It was found that shear stress applied during crystallization shifted peak temperature to higher temperature and broadened peak of bulk crystallization rate. It should be noted here that the values of  $(t_{0.5^{-1}})_0$  and  $K_g$  used were  $1.15 \times 10^5 \text{ min}^{-1}$ , and  $1.73 \times 10^5 \text{ K}^2$  (regime III), respectively, were used to plot the curve of bulk crystallization rate of zero shear stress. Guo and Narh [6] also showed the effect of shear stress on crystallization constant of PET and used the values of  $(t_{0.5^{-1}})_0$  and  $K_g$  from literature but they did not mention that which regime these values fall. They also suggested that the change in crystallization rate peak from quiescent crystallization to stress-induced crystallization is much faster in a slow crystallizing polymer (i.e., PET) than in a fast crystallizing polymer (i.e., i-PP). For shear-induced crystallization using cone and plate rheometer in this work, the crystallization temperature used was in the range of

regime II as mentioned previously (ca.  $T_c > 200^\circ\text{C}$ ) to obtain full curve of bulk crystallization rate. Using the value of  $(t_{0.5}^{-1})_0$  and  $K_g$  from regime II should also show the same trend. It was found that shear stress applied during crystallization can increase bulk crystallization rate. The shape of curve was found to be broader and the peak temperature was shifted to higher temperature.

### 4.3. Isothermal Crystallization from the Melt of Shear Treated Samples

The sheared samples which prepared using capillary rheometer with shear rate  $245.6 \text{ s}^{-1}$  and  $268.0 \text{ s}^{-1}$  at shearing temperature  $T_s$  250 and  $260^\circ\text{C}$  for 5 min were also used to study isothermal melt crystallization. It should be note here that the difference of shear rate is negligible so we assumed that it is at the same shear rate. The comparison of the values of reciprocal half-times of crystallization  $t_{0.5}^{-1}$  is shown in Figure 3. It is well known that  $t_{0.5}^{-1}$  can be referred to bulk crystallization rate of polymer. It was found that PTT shear treated sample at  $T_s$   $250^\circ\text{C}$  showed a higher rate of crystallization than that at  $T_s$   $260^\circ\text{C}$  and neat PTT samples. It can be explained that lower shearing temperature should have higher molecular orientation which still remain after melting at fusion temperature before isothermal melt crystallization. It should be noted here that the effect of residual crystallites may contribute at lower shearing temperature. Avrami model as shown in Equation (1) was also used to analyzed isothermal data of shear untreated and shear treated PTT samples within crystallization temperature ranging from ca.  $190$  to  $200^\circ\text{C}$  and summarized in Table 3. Avrami exponent  $n_a$  of neat PTT was less higher than that of both shear treated samples at different  $T_s$ . The Avrami exponent  $n_a$  was found ranging from 1.96 to 2.29 for neat PTT, 1.44 to 1.69 for shear treated PTT at  $T_s$   $250^\circ\text{C}$ , and 1.61 to 1.83 for shear treated PTT at  $T_s$   $260^\circ\text{C}$ , respectively. The Avrami crystallization rate  $K_a$  of sheared sample at  $T_s$   $250^\circ\text{C}$  was highest following by shear treated sample at  $T_s$   $260^\circ\text{C}$  and neat PTT, respectively, at the same  $T_c$ . Figure 4 also illustrates plot of  $\log(t_{0.5}^{-1}) + U^*/2.303R(T_c - T_\infty)$  versus  $1/2.303T_c(\Delta T)f$  of shear treated samples at different shearing temperature. It was found that the results of sheared sample should fall in regime III because the change of slope cannot be observed in temperature range studied. The values of  $(t_{0.5}^{-1})_0$  found to be ca.

$1.03 \times 10^5$  and  $4.86 \times 10^4 \text{ min}^{-1}$  for sheared sample at  $T_s$  250 and 260°C, respectively. The values of  $K_g$  found to be ca.  $1.42 \times 10^5$  and  $1.47 \times 10^5 \text{ K}^2$  for sheared sample at  $T_s$  250 and 260°C, respectively. The values of  $(t_{0.5^{-1}})_0$  and  $K_g$  of both sheared PTT samples at different shearing temperature were lower than that of neat PTT sample. Based on modified differential Nakamura model proposed by Ahn et al. [5], non-linear regression method was used to fit the value of reciprocal crystallization half-time  $t_{0.5^{-1}}$  of shear treated samples at different  $T_s$  at 250 and 260°C by using the value of  $(t_{0.5^{-1}})_0$  from isothermal crystallization in quiescent condition. The value of nucleation exponent  $K_g$  calculated of shear treated samples was also called nucleation exponent due to orientational effect  $K_{g,0}$  and was also used to determine the value of degree of orientation that was equal to  $(K_g/K_{g,0})-1$ . The value of  $K_{g,0}$  were  $1.44 \times 10^5$  and  $1.66 \times 10^5 \text{ K}^2$  for PTT shear treated sample at  $T_s$  250 and 260°C, respectively (kept the difference of shear rate used to minimum). The value of  $h(T, \tau)$  at  $T_s$  250°C shown the higher value than that at  $T_s$  260°C (i.e.,  $h(T, \tau) = 0.201$  and  $0.042$  for  $T_s$  250 and 260°C, respectively).

#### 4.4. Non Isothermal Crystallization from the Melt of Shear Untreated and Shear Treated Sample

The non-isothermal crystallization process can be considered as a combination of finite steps of isothermal crystallization process. Thus, the non-isothermal crystallization process can be predicted by using parameters from the isothermal crystallization kinetics. Figure 8 illustrates the comparison between the predicted results of non-isothermal crystallization data of PTT various cooling rate by using differential Nakamura model (Equation (4)) by using isothermal parameters and directly fitting. Marquardt's non-linear regression analysis [17] was used to fit the non-isothermal experimental data. It was found that using directly fitting method gave better results than using parameters from isothermal crystallization (using  $(t_{0.5^{-1}})_0$  and  $K_g$  from regime III because all of melt crystallization peak occurred when temperature lower ca. 200°C). For PTT samples studied, using isothermal parameters fitted well only at lowest cooling rate (i.e.  $5^\circ\text{C}\cdot\text{min}^{-1}$ ). In this work, the non-isothermal data can be fitted using  $n$ ,  $(t_{0.5^{-1}})_0$ , and  $K_g$  as parameters of model

while keeping  $U^* = 1500\text{cal}\cdot\text{mol}^{-1}$ . The values of parameters  $n$ ,  $(t_{0.5}^{-1})_0$ , and  $K_g$  of neat PTT are listed in Table 2. The model of Patel and Spruiell [2] was also used to fit experimental data comparing with original differential Nakamura model.

#### 4.5. Non-Isothermal Crystallization from the Melt of Sheared samples

The sheared samples were prepared using capillary rheometer with shear rate  $92.1\text{ s}^{-1}$  and  $245.6\text{ s}^{-1}$ . we assume that sheared samples should still retained some orientation although melting at fusion temperature. The experiment was similar to the case of quiescent non-isothermal melt crystallization. Figure 9 illustrates crystallization exotherms of shear untreated and shear treated sample at  $92.1$  and  $245.6\text{ s}^{-1}$ , respectively, with various heating rates  $10, 20, 30,$  and  $40^\circ\text{C}\cdot\text{min}^{-1}$ . The peak temperature of melt crystallization  $T_{\text{cm}}$  was shifted to the lower temperature as cooling rate increased for both shear untreated and shear treated samples. At the same cooling rate, the position of  $T_{\text{cm}}$  of sheared sample was located at higher temperature than that of non-sheared sample and shifted little to the lower temperature as shear rate increased. The shift of position of  $T_{\text{cm}}$  of sheared sample should be attributed to the molecular orientation which still remain in melt state. Table 2 also summarizes the effect of cooling rate on the crystallization kinetics parameters  $n$ ,  $(t_{0.5}^{-1})_0$  and  $K_g$  obtained from fitting the experimental data. Figure 10 also illustrates the effect of cooling rate on the degree of orientation calculated in which shear stress were  $2.99\times 10^4$  and  $6.62\times 10^4$  Pa for shear treated samples at  $92.1$  and  $245.6\text{ s}^{-1}$ , respectively. Based on modified Nakamura model which accounts the effect of shear [2] by keeping the value of  $(t_{0.5}^{-1})_0$  from quiescent condition as constant in the model of shear-induced crystallization kinetics. The value of degree of orientation  $h(T, \tau)$  were not strongly dependent on cooling rate increased and  $h(T, \tau)$  at higher shear rate shown the higher value at almost heating rate.

#### 4.6. Effective Activation Energy Describing the Overall Crystallization Process

The plots of effective activation energy  $\Delta E$  of PTT non-sheared and sheared sample as a function of melt conversion based on the Friedman method [14] are presented in Figure 10. Table 4 also summarizes the values of the effective

activation energy  $\Delta E$  for these PTT samples. It is apparent that the effective activation energy of neat PTT, PTT sheared sample at 92.1 and 245.6 s<sup>-1</sup> increases with increasing melt conversion  $\alpha$ . Both sheared samples show lower value of activation energy at all melt conversions which means that requiring the lower activation energy for transportation of molecular segment from the molten state to the crystal growth surface as a function of melt conversion increases.

## 5. CONCLUSIONS

In-situ shear-induced isothermal melt crystallization was investigated using cone and plate rheometer. At the same crystallization temperature, the induction time was found to decrease with increasing shear rate. As shear stress increased, the temperature shift was increased exponentially. Shear stress applied during crystallization can also increase bulk crystallization rate and shift peak temperature to higher temperature. For shear treated sample from capillary rheometer, PTT sheared sample prepared at lower shearing temperature gave a higher rate of crystallization than that at higher shearing temperature and neat PTT samples. For non-isothermal crystallization from melt of neat PTT, fitting the experimental data using directly fitting give a better result than using parameter from quiescent crystallization. The position of melt crystallization peak was found to be located at higher temperature as shear rate increased at a fixed cooling rate. The activation energy required for transportation of molecular segment from the molten state to the crystal growth surface of shear treated samples was found to be lower than that of shear untreated sample at all melt conversion calculated.

## 6. ACKNOWLEDGMENTS

The authors wish to thank Dr. Hoe H. Chuah and his co-workers of Shell Chemical Company (USA) Ltd. for supply of PTT and for their kind assistance on molecular weight measurements on PTT resins received. PS acknowledges a grant provided by Chulalongkorn University through the Development Grants for New Faculty/Researchers. Partial in-kind support from the Petroleum and Petrochemical College is also greatly acknowledged.

**REFERENCES**

- [1] Wolkowicz MD, Ph.D. Dissertation in Polym Sci Eng 1983, Graduate school, University of Massachusetts.
- [2] Patel MR and Spruiell JE, Polym Eng Sci 1991, 31, 730.
- [3] Eder G, Janeschitz-Kriegl H, Lidauer S, Progress Polym Sci 1990, 15, 629.
- [4] Jerschow P and Janeschitz-Kriegl H, Int Polym Proc 1997, 12, 72.
- [5] Ahn SH, Cho CB, and Lee KY, J Reinf Plas and Comp 2002, 21, 617.
- [6] Guo J and Narh KA, Adv PolymTech 2002, 21, 214.
- [7] Chuah H, in John Scheirs and Timothy Long ed. "Modern Polyester", John Wiley.
- [8] Avrami M, J Chem Phys 1939, 7, 1103.
- [9] Avrami M, J Chem Phys 1940, 8, 212.
- [10] Avrami M, J Chem Phys 1941, 9, 177.
- [11] Godovsky YK and Slonimsky GL, J App Polym Sci 1974, 12, 1053.
- [12] Nakamura K, Katayama K, Amano T, J App Polym Sci 1973, 17, 1031.
- [13] Hoffman JD, Davis GT, Lauritzen JI Jr, in: N.B. Hannay (Ed.), Treatise on Solid state Chemistry, Vol. 3, Plenum Press, Newyork, 1976, Chapter 7.
- [14] Friedman, J Polym Sci C 1964-1965, 6, 183.
- [15] Hass TW, Maxwell B, Polym Eng Sci 1969, 9, 226.
- [16] Dangseeyun N, Srimoaoon P, Supaphol P, and Nithitanakul M, Thermochim Acta, submitted.
- [17] Constantinides A and Mostoufi N, In "Numerical Methods for Chemical Engineers with MATLAB Applications", Prentice Hall PTR, New Jersey 1999, 507.

**CAPTION OF TABLES**

- Table 1 Induction time and equilibrium melting temperature of PTT samples with different crystallization temperature and shear rate
- Table 2 Crystallization kinetic parameters for PTT samples based on Differential Nakamura and Modified Differential Nakamura model
- Table 3 Overall crystallization kinetic data for PTT samples based on Avrami model
- Table 4 Effective activation energy  $\Delta E$  describing the overall crystallization process of shear untreated and shear treated PTT samples based on Friedman method



## CAPTIONS OF FIGURES

- Figure 1 Induction time  $t_i$  as a function of crystallization temperature  $T_c$  of PTT samples.
- Figure 2 Plot of  $\log t_i$  against  $\log(T_m^0 - T_c)$  for various choice of crystallization temperature  $T_c$  ranging from 198 to 213°C.
- Figure 3 Reciprocal half-time as a function of crystallization temperature of PTT samples
- Figure 4 Analysis of the half-times of crystallization based on the modified growth rate theory for the PTT samples.
- Figure 5 Shear stress as a function of shearing time at crystallization temperature  $T_c$  210°C with different shear rate 1 and 3  $s^{-1}$ .
- Figure 6 Equilibrium melting temperature shift as a function of shear stress, solid line shown the result of fitting data.
- Figure 7 Bulk crystallization rate as a function of temperature with various shear stress applied during crystallization of PTT samples.
- Figure 8 Relative crystallinity as a function of neat PTT with different cooling rates. The fitting results using differential Nakamura model and isothermal parameters is shown as dash and solid line, respectively.
- Figure 9 Non-isothermal melt crystallization exotherms of PTT samples at shear rate 0, 92.1 and 245.6  $s^{-1}$  at different four cooling rates.
- Figure 10 Degree of orientation  $h(T, \tau)$  as a function of shear stress for PTT shear treated sample at 92.1 and 245.6  $s^{-1}$  at different four cooling rate.
- Figure 11 Determination of the effective activation energy  $\Delta E$  as a function of melt conversion  $\alpha$  describing the overall crystallization process for PTT samples at shear rate 0, 92.1, and 245.6  $s^{-1}$  based on Friedman method.

**Table 1** Induction time and equilibrium melting temperature of PTT samples with different crystallization temperature and shear rate

$T_c$ °C	Shear Rate s <sup>-1</sup>	Shear Stress Pa	$t_i$ s	$T_{m}^{shif}$ °C
210	0	-	213	-
	1	210	130	2.18
	3	940	60	5.82
	5	1440	40	7.87
211	0	-	253	-
	1	150	200	1.31
	3	475	140	2.85
	5	880	75	5.73
212	0	-	341	-
	1	169	230	1.72
	3	642	115	4.74
	5	790	120	4.54

**Table 2** Crystallization kinetic parameters for PTT samples based on Differential Nakamura and Modified Differential Nakamura model

Fitting with differential Nakamura model													
Shear Rate (s-1)		0				92.1				245.6			
$\phi$ °C·min <sup>-1</sup>	<i>n</i>	(1/ <i>t</i> <sub>0.5</sub> ) <sub>0</sub> min <sup>-1</sup>	<i>K<sub>g</sub></i> <i>K</i> <sup>2</sup>	<i>r</i> <sup>2</sup>	<i>n</i>	(1/ <i>t</i> <sub>0.5</sub> ) <sub>0</sub> min <sup>-1</sup>	<i>K<sub>g</sub></i> <i>K</i> <sup>2</sup>	<i>r</i> <sup>2</sup>	<i>n</i>	(1/ <i>t</i> <sub>0.5</sub> ) <sub>0</sub> min <sup>-1</sup>	<i>K<sub>g</sub></i> <i>K</i> <sup>2</sup>	<i>r</i> <sup>2</sup>	
10	2.22	1.82×10 <sup>5</sup>	1.87×10 <sup>5</sup>	0.9999	1.45	2.98×10 <sup>5</sup>	1.79×10 <sup>5</sup>	0.9983	1.78	1.13×10 <sup>5</sup>	1.60×10 <sup>5</sup>	0.9954	
20	2.29	9.64×10 <sup>4</sup>	1.73×10 <sup>5</sup>	0.9999	1.74	1.06×10 <sup>5</sup>	1.63×10 <sup>5</sup>	0.9988	2.07	1.04×10 <sup>5</sup>	1.50×10 <sup>5</sup>	0.9984	
30	2.74	5.41×10 <sup>4</sup>	1.63×10 <sup>5</sup>	0.9998	1.77	8.40×10 <sup>4</sup>	1.58×10 <sup>5</sup>	0.9983	1.80	1.23×10 <sup>5</sup>	1.58×10 <sup>5</sup>	0.9980	
40	2.99	8.02×10 <sup>4</sup>	1.69×10 <sup>5</sup>	1.000	2.19	9.98×10 <sup>4</sup>	1.59×10 <sup>5</sup>	0.9993	1.96	9.73×10 <sup>4</sup>	1.53×10 <sup>5</sup>	0.9979	

Fitting with modified differential Nakamura model													
Shear Rate (s-1)		0				92.1				245.6			
$\phi$ °C·min <sup>-1</sup>	<i>n</i>	(1/ <i>t</i> <sub>0.5</sub> ) <sub>0</sub> min <sup>-1</sup>	<i>K<sub>g</sub></i> <i>K</i> <sup>2</sup>	<i>r</i> <sup>2</sup>	<i>n</i>	(1/ <i>t</i> <sub>0.5</sub> ) <sub>0</sub> min <sup>-1</sup>	<i>K<sub>g</sub></i> <i>K</i> <sup>2</sup>	<i>r</i> <sup>2</sup>	<i>n</i>	(1/ <i>t</i> <sub>0.5</sub> ) <sub>0</sub> min <sup>-1</sup>	<i>K<sub>g</sub></i> <i>K</i> <sup>2</sup>	<i>r</i> <sup>2</sup>	
10	3.00	9.07×10 <sup>4</sup>	6.68×10 <sup>4</sup>	0.9972	1.30	1.50×10 <sup>7</sup>	1.65×10 <sup>5</sup>	0.9962	1.07	2.71×10 <sup>5</sup>	1.76×10 <sup>5</sup>	0.9856	
20	2.05	6.07×10 <sup>4</sup>	1.60×10 <sup>5</sup>	0.9975	1.42	7.94×10 <sup>5</sup>	2.13×10 <sup>5</sup>	0.9908	1.47	1.30×10 <sup>5</sup>	1.53×10 <sup>5</sup>	0.9926	
30	2.55	3.99×10 <sup>5</sup>	2.20×10 <sup>5</sup>	0.9977	1.30	7.29×10 <sup>5</sup>	2.03×10 <sup>5</sup>	0.9844	1.31	5.65×10 <sup>5</sup>	1.95×10 <sup>5</sup>	0.9918	
40	2.65	1.03×10 <sup>5</sup>	1.73×10 <sup>5</sup>	0.9986	1.78	2.00×10 <sup>5</sup>	1.76×10 <sup>5</sup>	0.9982	1.31	1.23×10 <sup>6</sup>	2.17×10 <sup>5</sup>	0.9921	

**Table 3** Overall crystallization kinetic data for PTT samples based on Avrami model

$T_c$ °C	$t_{0.5}^{-1}$ min <sup>-1</sup>	$K_a$ min <sup>-1</sup>	$n_a$	$r^2$
Neat PTT				
190	1.11	0.940	2.12	0.9999
192	0.953	0.792	1.96	0.9999
194	0.743	0.626	2.03	0.9998
196	0.639	0.549	2.29	0.9998
198	0.464	0.387	2.00	0.9999
200	0.337	0.294	2.40	0.9992
PTT Shear Rate 245.6s <sup>-1</sup> T <sub>a</sub> 250°C				
192	2.92	2.31	1.69	0.9986
194	2.45	1.96	1.69	0.9995
196	1.98	1.52	1.44	0.9968
198	1.71	1.34	1.61	0.9984
200	1.33	1.04	1.60	0.9966
PTT Shear Rate 268.0 s <sup>-1</sup> T <sub>a</sub> 260°C				
190	1.35	1.11	1.83	0.9998
192	1.053	0.728	1.82	0.9993
195	0.741	0.600	1.73	0.9999
198	0.637	0.516	1.73	0.9999
200	0.49	0.389	1.61	0.9997

**Table 4** Effective activation energy  $\Delta E$  describing the overall crystallization process of shear untreated and shear treated PTT samples based on Friedman method

Shear Rate $s^{-1}$	Activation Energy $\Delta E$ ( $\text{kJ mol}^{-1}$ )				
	$\alpha = 0.1$	$\alpha = 0.3$	$\alpha = 0.5$	$\alpha = 0.7$	$\alpha = 0.9$
0	-104.1	-94.3	-87.2	-85.9	-83.8
92.1	-131.0	-125.4	-119.3	-114.2	-88.8
245.6	-136.0	-125.2	-118.4	-113.9	-100.5

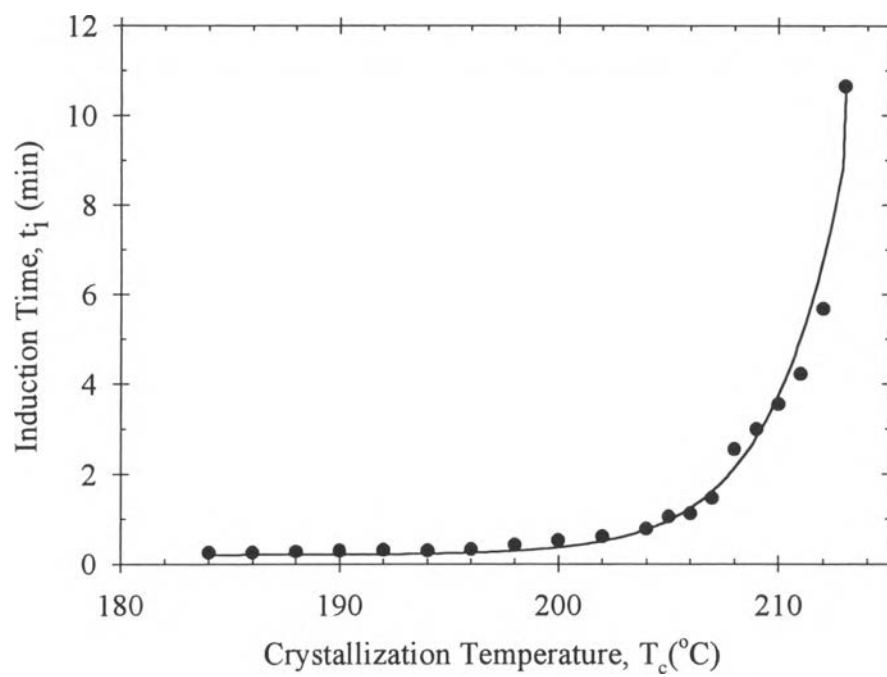


Figure 1

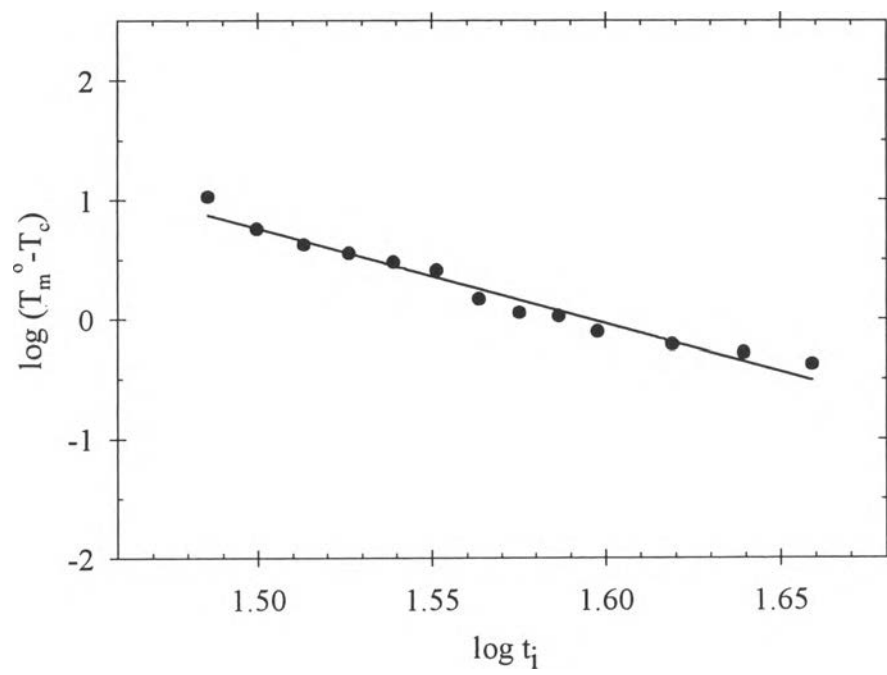


Figure 2

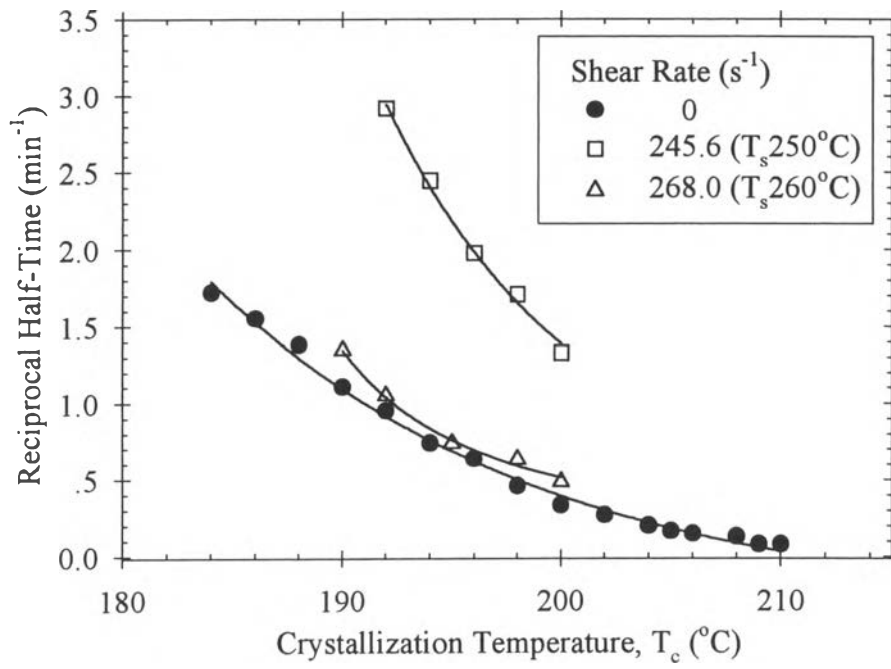


Figure 3



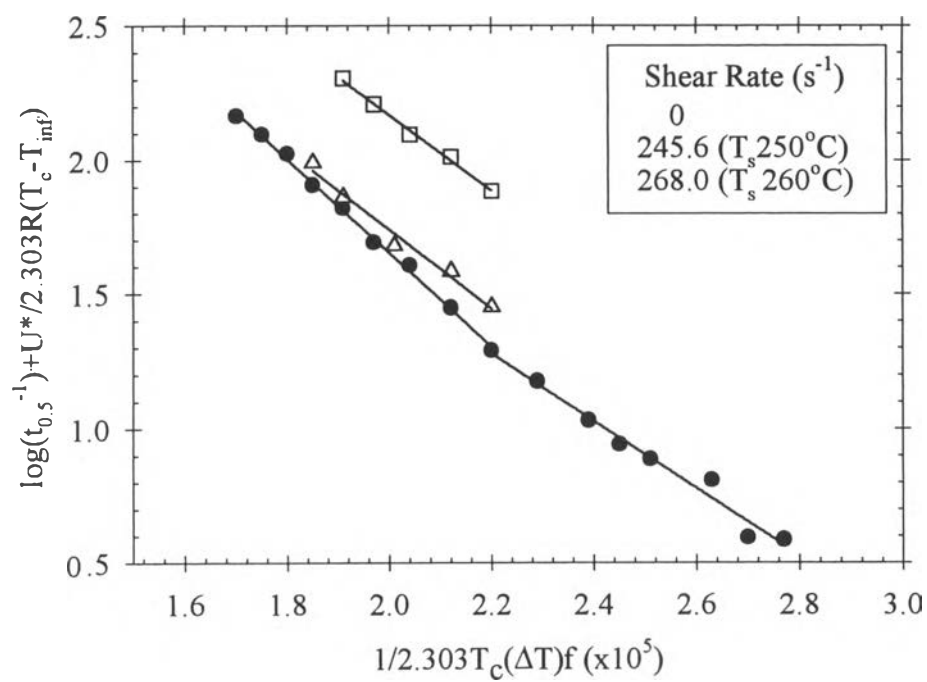


Figure 4

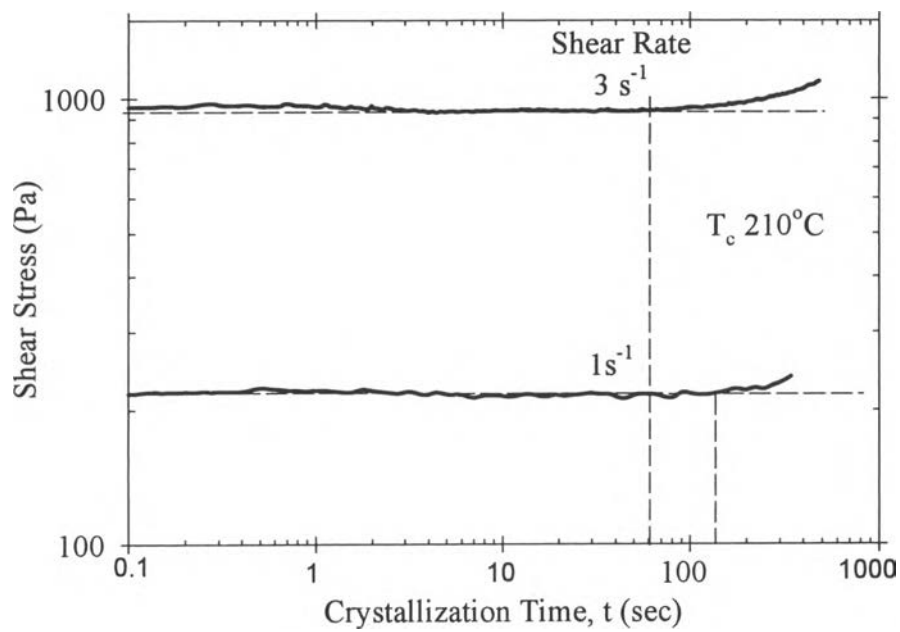


Figure 5

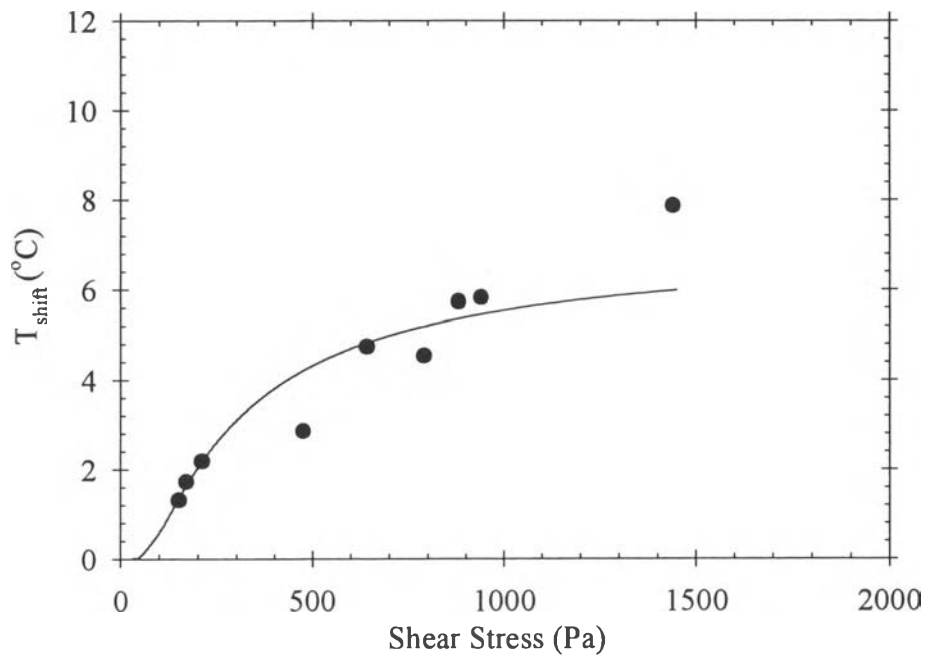


Figure 6

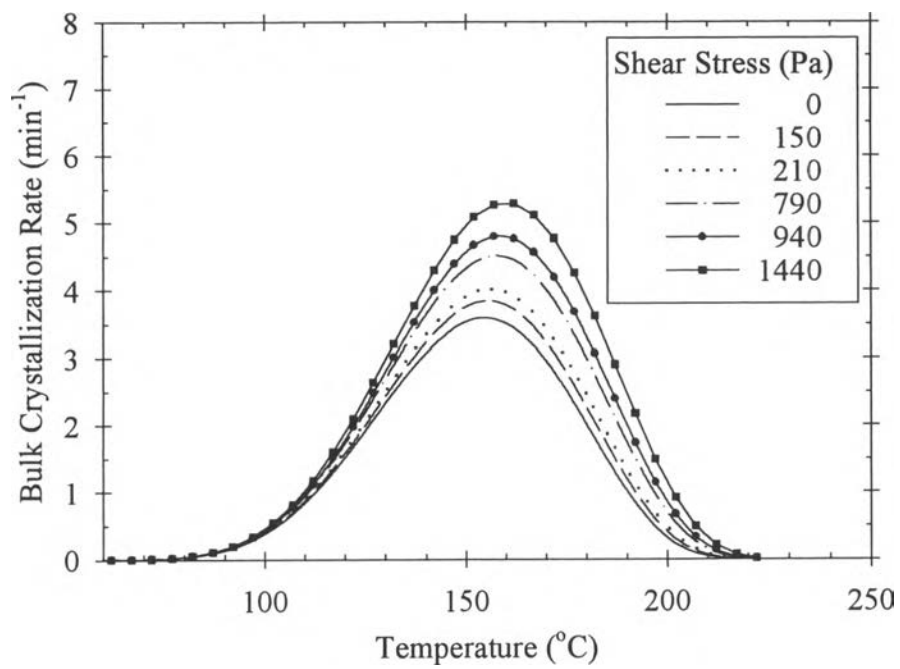


Figure 7

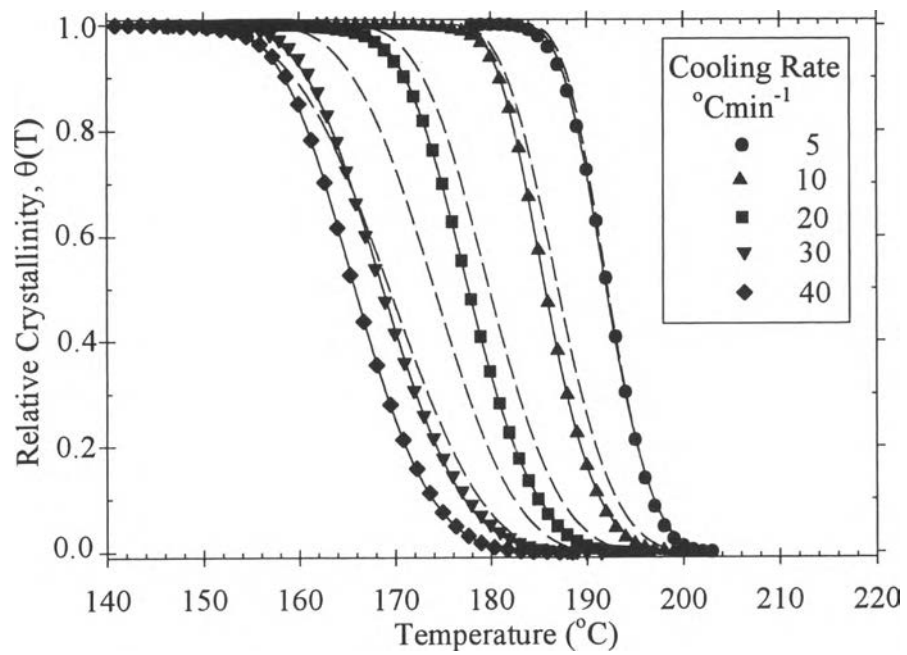


Figure 8

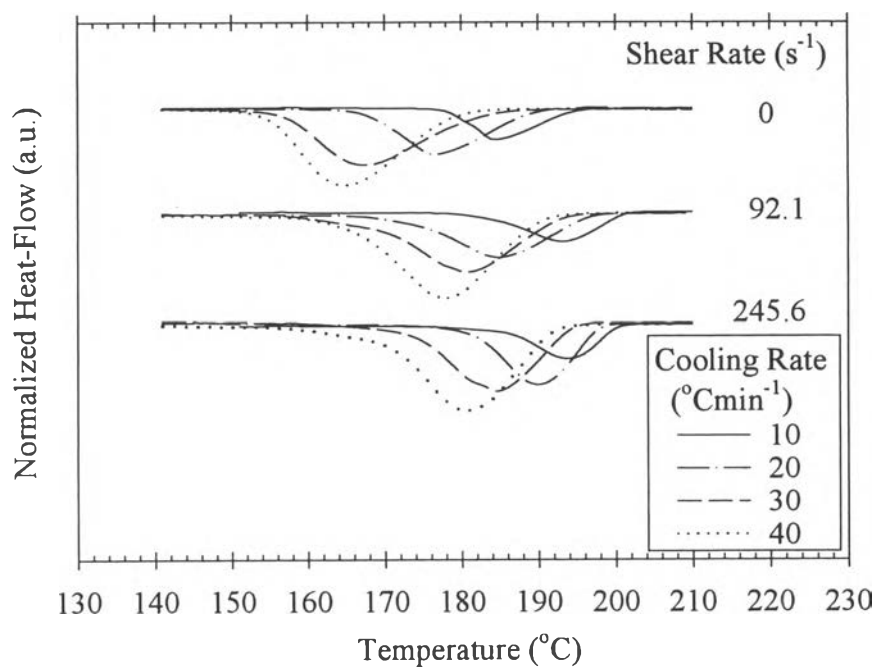


Figure 9

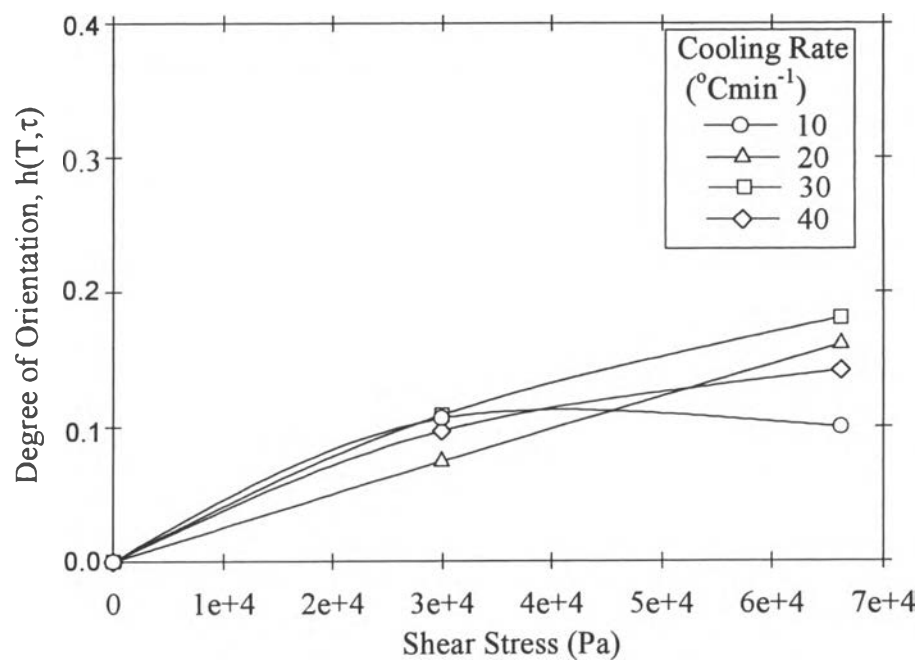


Figure 10

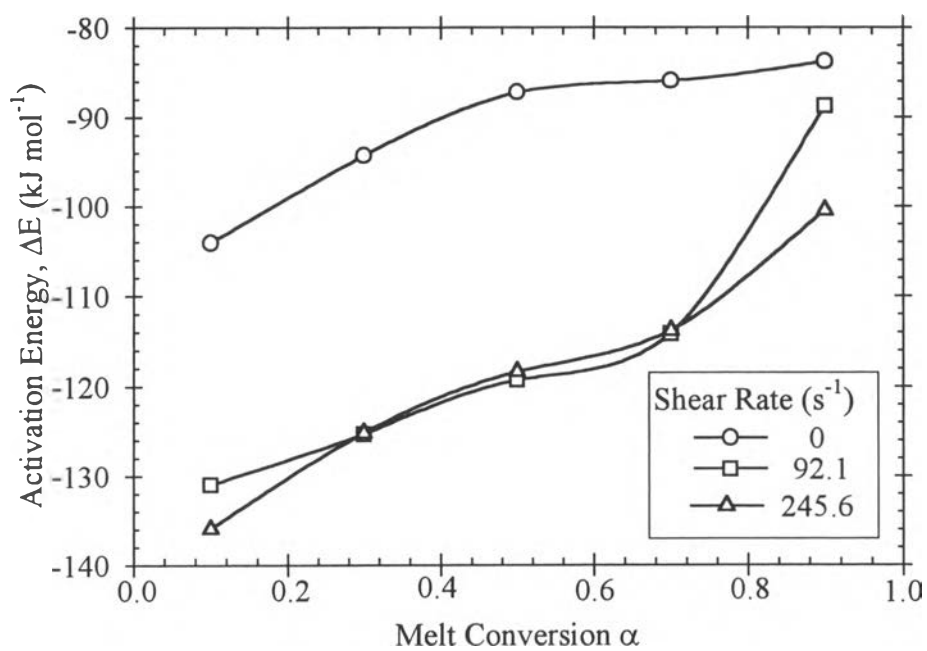


Figure 11